PERGAMON

Marine Pollution Bulletin 45 (2002) 332–338

MARINE POLLUTION BULLETIN

www.elsevier.com/locate/marpolbul

Mathematical modeling of PCB bioaccumulation in *Perna viridis*

K.N. Yu [a,b,*], P.K.S. Lam [b,c], C.C.C. Cheung [b,c], C.W.Y. Yip [a]

[a] *Department of Physics and Materials Science, City University of Hong Kong, Tat Chee Avenue, Kowloon Tong, Kowloon, Hong Kong*
[b] *Centre for Coastal Pollution and Conservation, City University of Hong Kong, Tat Chee Avenue, Kowloon Tong, Kowloon, Hong Kong*
[c] *Department of Biology and Chemistry, City University of Hong Kong, Tat Chee Avenue, Kowloon Tong, Kowloon, Hong Kong*

Abstract

In the present work, we built a mathematical model of polychlorinated biphenyl (PCB) bioaccumulation in *Perna viridis*, namely, a one-compartment model with a time dependent incorporation rate R ($\mu g\,g^{-1}$ lipid per ppb water per day), with positive substrate cooperativity as the underlying physical mechanism. The temporal change of the PCB concentration Q ($\mu g\,g^{-1}$ lipid) in the soft tissues of the mussel depends on the competition of the input rate RW and the output rate kQ, where W is the concentration of PCB in water (ppb water) and k is the elimination rate (per day). From our experimental data, $k = 0.181 \pm 0.017\ d^{-1}$. The critical concentration in water W_c for positive substrate cooperativity was found to be ~2.4 ppb. Below W_c, R is a constant. For a water concentration of 0.5 ppb Aroclor 1254, $R = 24.0 \pm 2.4\ \mu g\,g^{-1}$ lipid $ppb^{-1}\,d^{-1}$. Above W_c, positive substrate cooperativity comes into effect and R becomes a function of time and dependent on the concentration Q in a form $R = \gamma Q/(Q + \delta)$. This is the case for a water concentration of 5 ppb Aroclor 1254, where $\gamma = 15.1\ \mu g\,g^{-1}$ lipid $ppb^{-1}\,d^1$ and $\delta \approx 200\ \mu g\,g^{-1}$ lipid. From this model, the uptake is exponentially increasing when the PCB concentration in the mussel is small compared to 200 $\mu g\,g^{-1}$ lipid, and hyperbolically increasing when the concentration is large compared to 200 $\mu g\,g^{-1}$ lipid, which are consistent with the experimental data. The model is useful for understanding the true processes taking place during the bioaccumulation and for risk assessment with higher confidence. Future experimental data which challenge the present model are anticipated and in fact desirable for improvement and perfection of the model.

1. Introduction

Although the sale and use of polychlorinated biphenyls (PCBs) have been banned in most countries for almost 20 years, PCB congeners and related polyhalogenated hydrocarbons still pose a serious threat to aquatic organisms. Connell et al. (1998a,b) reviewed the environmental risks associated with chlorinated hydrocarbons in Hong Kong waters and concluded that organochlorines, including PCBs, could pose significant risks to the local marine ecosystem (Zheng et al., 2000).

Mussels are filter feeders and may accumulate particulate-bound pollutants. Trace organic contaminants, such as PCBs, tend to be distributed in higher concentrations in the particulate phase, and may accumulate in mussel tissues to relatively high levels as a result of a dynamic process between the uptake and depuration process. Mussels have been used in many parts of the world as indicator organisms because of their ability to accumulate environmental contaminants especially lipophilic compounds such as petroleum hydrocarbons, chlorinated pesticides, polycyclic aromatic hydrocarbons (PAHs) and PCBs (e.g. Martin, 1992; Sericano et al., 1995; Richardson et al., 2001). DNA adduct formation in *Perna viridis* has been found to be associated with exposure to genotoxic PAHs (Xu et al., 1999), while the antioxidative responses in the mussels were associated with PAHs (Cheung et al., 2001) and chlorinated hydrocarbons (PCBs and chlorinated pesticides) (Cheung et al., in press). These findings suggest that tissue concentrations of persistent organic contaminants may be a good predictor of biomarker responses, which potentially may have an effect at cellular, individual or even population levels.

In tropical/subtropical Asia, the green-lipped mussels, *Perna viridis* (Linnaeus, 1758) (Bivalvia: Mytilacea), have been suggested to be useful organisms for moni-

* Corresponding author. Address: Department of Physics and Materials Science, City University of Hong Kong, Tat Chee Avenue, Kowloon Tong, Kowloon, Hong Kong. Tel.: +852-2788-7812; fax: +852-2788-7830.
E-mail address: peter.yu@cityu.edu.hk (K.N. Yu).

0025-326X/02/$ - see front matter © 2002 Elsevier Science Ltd. All rights reserved.
PII: S0025-326X(02)00099-1

toring conservative contaminants, including metals and trace organic contaminants (Phillips, 1985, 1989; Tanabe et al., 1987).

Recent studies have demonstrated that it may be possible to predict toxicant loading, for certain metals, in specific organs/tissues of the target organisms using simple first-order biokinetic dynamic models, provided that the exposure, albeit fluctuating, regime is known (Yu et al., 2000). This ability to predict tissue toxicant concentrations would mean that it is possible, at least in principle, to predict biomarker responses (provided that the relationship between biomarker responses and tissue toxicant concentrations has been established) or, through extrapolation, biological effects at higher levels of biological organization. Theoretically, this would allow a preliminary assessment of potential biological effects from concentration data of target contaminants in the environment over time. Indeed, Lam and Gray (2001) suggested that it might be possible to use dynamic kinetic models to predict tissue toxicant loading in organisms exposed to fluctuating environmental concentrations, and to use the tissue toxicant loading so calculated in establishing dose-response relationships.

In the present investigation, we attempt to build a mathematical model of PCB bioaccumulation in *P. viridis*. The simplest and easiest model will always be an empirical model. However, for understanding the true processes taking place and for risk assessment with higher confidence, models with realistic underlying physical mechanisms are more desirable. Our strategy is to identify the simplest model with a reasonable physical mechanism which can explain the experimental data. In Section 2, we will first present details of our experiments as well as the results. In Section 3, we will then describe the procedures to build our mathematical model. As adopted by Yu et al. (2000), the simplest way is to adopt first-order biokinetic dynamic models, i.e., to assume all uptake and depuration processes to be governed by first order linear differential equations. As a first trial, we treat the soft tissue as a single-compartment (single-compartment model). Of course, this simplest single-compartment model with first order kinetics might not apply to all situations. We will see in Section 3 why such a model fails to describe the PCB bioaccumulation in *P. viridis*. More complicated variants of this models are then explored, and the simplest one which can satisfactorily describe the experimental data will be finally presented.

This final model will be taken as our best model at the moment. In future, experimental data might be generated to challenge the established model. These challenges are anticipated and in fact desirable for improvement and perfection of the model. Without the first-version model, however, challenges will never appear and the true model will never be revealed. The objective of the present paper is therefore an attempt to establish this first-version model.

2. Experimental

2.1. Laboratory exposure experiment

Individuals of green-lipped mussel, *P. viridis* (L.) were collected from Kat O Fish Farm, NE of Hong Kong. They were brought back to the laboratory and had the epibionts removed. Mussels with shell lengths between 90 and 110 mm were selected and acclimatized in a flow-through system with natural seawater for 10 d. During this period, a unicellular green alga, *Dunaliella tertiolecta*, was given daily as food. Seawater was changed daily and dead mussels were immediately removed and discarded.

30-l glass aquaria were used as test containers in the exposure experiment. The inner surface of each container was first cleaned with acetone and then hexane and dichloromethane. The mussels were exposed to two nominal concentrations of Aroclor 1254 (0.5 and 5 $\mu g\,l^{-1}$) pre-dissolved in acetone. Seawater containing acetone only served as the solvent control, while the control groups consisted of mussels in filtered seawater. Each exposure tank contained 20-l of sand-filtered seawater and 10 mussels. The experimental conditions were: temperature: 25 ± 1 °C; salinity: $32° \pm 1‰$; pH: 7.8; DO: 7 ± 1 $mg\,l^{-1}$. The seawater has PCB levels below the detection limit of 1 $ng\,l^{-1}$.

Two exposure tanks were used per treatment. During the entire exposure period (18 d), seawater was changed daily after the mussels had been fed with a green alga, *D. tertiolecta*, at a constant cell density of 3×10^6 $cells\,l^{-1}$. The tanks were inspected regularly, and dead mussels were removed immediately and replaced by mussels of the similar size. Every six days, three mussels from each tank were randomly sampled for dissection. The mussel tissues were removed, weighed and stored at −20 °C for PCB analysis.

2.2. Extraction of organic contaminants from the mussel tissue

Briefly, the soft tissue of each mussel was freeze-dried and homogenized into fine powder by a tissue grinder. A recovery internal standard, 1,2,3,4,5,6,7,8-octachloronaphthalene, was added to each centrifuge tube and mixed with the mussel powder. The dried mussel powder was extracted in a 50 ml fluorinated ethylene propylene centrifuge tube, containing 30 ml distilled methylene chloride and 2 g of anhydrous sodium sulphate. The tube was then placed on a horizontal shaker and shook for 10 min and the extract was centrifuged at 3000*g* for 5 min to provide a supernatant. The extraction and centrifugation process was repeated twice, all three supernatants were combined (ca. 100 ml) and filtered through a glass fibre filter paper (GF/C grade). The solvent was exchanged into hexane through rotary evaporation of

the dichloromethane extract to about 5 ml, followed by the addition of hexane (30 ml) and by rotary evaporation again to about 1 ml. The volume of extract was subsequently reduced to dryness by nitrogen blowdown. Then the weight of the dried extract, taken as lipid weight, was measured. The dried extract was then redissolved by adding ~1 ml of distilled hexane and was ready to load onto a silica gel column for separation. A chromatography column of internal diameter of 1 cm with fused-in filter disc was used as fractionation column. It consists of 13 cm^3 of activated silica gel (average pore size: 60 Å) and 3 cm^3 of anhydrous sodium sulphate on the top (Prest et al., 1995).

The mussel extract was loaded to the silica gel column by using a Pasteur pipette. The mussel extract was allowed to penetrate into the sodium sulphate until the extract reached the surface of sodium sulphate. The column was then successively eluted with 7 ml of hexane and 8 ml of hexane and finally two aliquots of 20% dichloromethane in hexane (15 ml). The first 7 ml of hexane containing mainly lipids was discarded. The following 8 ml of hexane (referred to as Fraction 1 (F1); containing PAHs) was collected and kept in 16-ml vials. The two fractions eluted by 20% dichloromethane in hexane were combined to give Fraction 2 (F2) for analysis of Aroclor 1254.

2.3. PCB analysis

As the electron capture detector (ECD) is sensitive to dichloromethane, so dichloromethane was removed from F2 by adding about 30 ml of hexane to F2 and subsequent rotary evaporating to about 1 ml. PCB Analysis was undertaken using Hewlett Packard 5890 series II gas chromatograph equipped with an ECD. Automatic 1-μl injections of external standard and ready-to-inject samples were controlled by an HP 7673 automatic controller. A HP-5MS column was used for separating organochlorines. The flow rate of total flow, septum purge and anode purge was 40, 2.5 and 8 ml N_2/min respectively. The column head pressure was maintained at 12 psi. The oven temperature was set at 90 °C at the beginning (held for 2 min) and raised to 180 °C (held for 1 min) at a ramp rate of 20 °C/min and then to 270 °C (held for 20 min) at a ramp rate of 3 °C/min. Temperature of the injector and detector was maintained at 230 and 300 °C respectively. Injection was made in splitless mode with the split valve being closed for 1 min. All data were expressed as ng g^{-1} lipid weight (Zheng and Quinn, 1988). The detection limits in the above analytical procedures was 3 ng g^{-1} for Aroclor 1254. Samples were analyzed in batches which included a known standard from the National Institute of Standards & Technology (SRM 2974). The percentage recoveries of PCBs in spiked samples by the above method ranged between 81.3% and 107.8%. Concentrations were not corrected for recovery rates.

3. Results

The experimental data for the bioaccumulation of PCB in *P. viridis* are shown in Fig. 1. The control data were obtained from mussels kept in filtered seawater, while the solvent control data from mussels kept in seawater containing acetone. There was no statistically significant difference in the PCB dynamics between the control and solvent controls ($F = 0.51$, $P > 0.05$). There was, however, a significant decline (depuration) in PCB levels in these mussels over the experimental period ($F = 57.62$, $P < 0.01$). There was clear evidence of PCB uptake by mussels exposed to 5 ppb PCB with a maximum mean concentration of 408 μg g^{-1} observed after 12 d, then dropping to around 260 μg g^{-1} on day 18 (Fig. 1). Although PCB uptake in mussels exposed to 0.5 ppb was also apparent, PCB concentrations in the mussels reached a maximum of around 60 μg g^{-1} after six days, and then remained relatively stable throughout the rest of the exposure duration (Fig. 1). Overall, PCB uptake rates in mussels exposed to 5 ppb were significantly higher than those exposed to 0.5 ppb ($F = 69.02$, $P < 0.01$). The initial concentration of PCB in experimental mussels (time = 0 d) was 37 ± 5 μg g^{-1} lipid.

3.1. Mathematical modeling

3.1.1. Single-compartment model with uptake and depuration processes governed by first order linear differential equations

The simplest and most straightforward model is to treat the soft tissues of the mussel as a single compartment (Fig. 2) and to treat the uptake and depuration

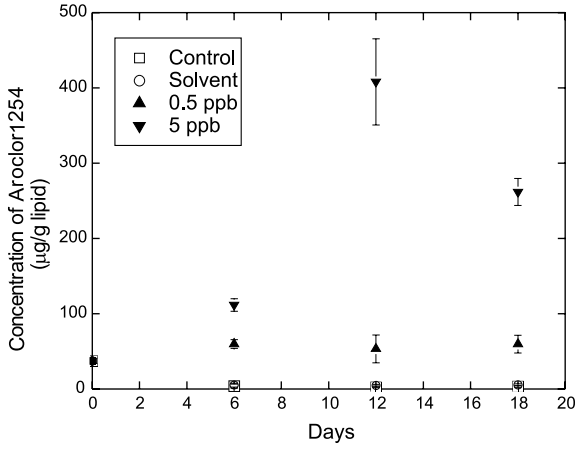

Fig. 1. Experimental results for the bioaccumulation of PCB in *P. viridis* (mean ±1 SD; n = 6).

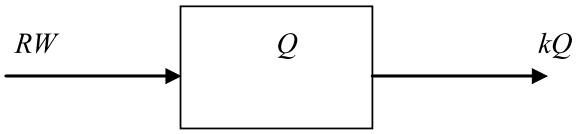

Fig. 2. Single-compartment model for the mussel.

processes as governed by first order linear differential equations. The uptake process is described by

$$\frac{dQ}{dt} = RW - kQ \tag{1}$$

where Q is the concentration of PCB in the soft tissues of the mussel ($\mu g\, g^{-1}$ lipid), W the concentration of PCB in water (ppb water), R the incorporation rate ($\mu g\, g^{-1}$ lipid per ppb water per day) and k is the elimination rate (per day). The solution to Eq. (1) is

$$Q = \frac{RW}{k}\left(1 - e^{-kt}\right) + Q_0 e^{-kt} \tag{2}$$

where Q_0 is the initial PCB concentration in the mussel (at $t = 0$ d). The depuration process can also be described by Eq. (1) with $RW = 0$ (i.e., zero intake), i.e.,

$$\frac{dQ}{dt} = -kQ \tag{3}$$

with the solution

$$Q = Q_1 e^{-k(t-t_1)} \tag{4}$$

where t_1 is the time when depuration starts and Q_1 is the PCB concentration in the soft tissues of the mussel at $t = t_1$. With known experimental values of W, Q_0 and Q_1, our tasks are then to determine the values of R and k from the experimental data both during the uptake and the depuration processes.

First we look at the depuration data (data for solvent control). They are apparently consistent with the depuration process described by Eq. (4). The data were fitted to Eq. (4) using the non-linear curve fitting option of Microcal™ Origin® (version 6.0), employing inverse of the variances as weights of the data. The elimination constant k was thus found to be 0.181 ± 0.017 d^{-1}.

We now look at the uptake data for the case of 0.5 ppb Aroclor 1254 in water. With the previously determined value of k, and by fitting the data to Eq. (2), RW should be obtainable. It is noted here that the curve generated by Eq. (2) is dominated by the first term on the right hand side of the equation, and the curve should thus be the well-known hyperbolic curve. Simply speaking, the curve should bend downwards and should saturate at large values of t. Employing the non-linear curve fitting option of Microcal™ Origin® and employing inverse of the variances as weights of the data, RW was found to be 12.0 ± 1.2 $\mu g\, g^{-1}$ lipid d^{-1} (or $R = 24.0 \pm 2.4$ $\mu g\, g^{-1}$ lipid ppb^{-1} d^{-1}).

From Eq. (2), we observe that the dimensionless equilibrium ratio between the concentrations of PCB in the soft tissues of the mussel ($\mu g\, g^{-1}$ lipid) and the concentration of PCB in water (ppb water) is given by (i.e., when $t \to \infty$) $K = Q/W(1000) = R/k(1000)$, where 1000 is the conversion from the unit $\mu g\, g^{-1}$ to the unit ppb. From the above results that $R = 24.0$ $\mu g\, g^{-1}$ lipid ppb^{-1} d^{-1} and $k = 0.181$ d^{-1}, we have $K \approx 133,000$. If the mussel is simply acting as a passive lipid receptor, the equilibrium ratio should be equal to the octanol–water partition, which for PCB1254 is somewhere between 6.3 and 6.5. Since the experimental accumulation is significantly higher, active transport should be responsible for the uptake.

We now turn to look at the uptake data for the case 5 ppb Aroclor 1254 in water. The initial plan was again to determine RW using the previously determined value of k in Eq. (2), and then by fitting the uptake data to Eq. (2). Unfortunately, however, the uptake data here were inconsistent with the uptake process described by Eq. (2). As mentioned above, the curve generated by Eq. (2) is hyperbolic, but the experimental data were clearly sigmoidal (bending upwards) instead of hyperbolic (bending downwards). Furthermore, the small variances of the data meant that the model described by Eq. (2), i.e., the single-compartment model with the uptake governed by first order linear kinetics can be rejected with high confidence. The following discussion will be devoted to developing more sophisticated models in order to better explain the experimental data.

3.1.2. Two-compartment models

The next simplest model (other than the single-compartment model) is the two-compartment model without recycling (Fig. 3), and treating the uptake and depuration processes as governed by first order linear differential equations. The uptake processes are then described by

$$\frac{dQ}{dt} = RW - (k_1 + \alpha)Q \tag{5}$$

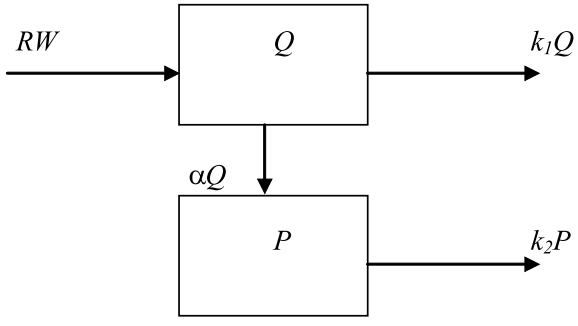

Fig. 3. Two-compartment model (without recycling) for the mussel.

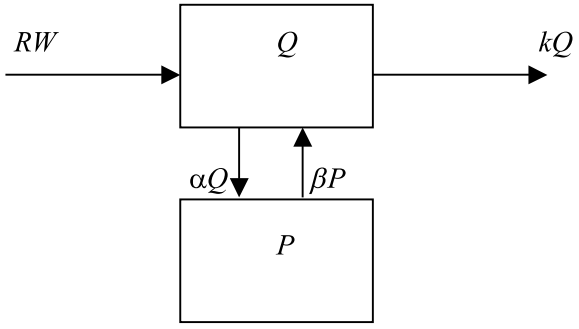

Fig. 4. Two-compartment model (with recycling) for the mussel.

and

$$\frac{dP}{dt} = \alpha Q - k_2 P \tag{6}$$

where k_1 and k_2 are the elimination rates (d^{-1}) from the first and second compartments, respectively, and α is the transfer rate (d^{-1}) from the first compartment to the second compartment. Unfortunately, the solutions to Eqs. (5) and (6) will also generate hyperbolic curves instead of sigmoidal curves. Therefore, the two-compartment model without recycling can also be rejected by the experimental data with high confidence.

When we discuss the two-compartment model, it is also natural to consider recycling as shown in Fig. 4. We can still treat the uptake and depuration processes as first order linear kinetics. The uptake processes are then described by the coupled differential equations:

$$\frac{dQ}{dt} = RW - (k + \alpha)Q + \beta P \tag{7}$$

$$\frac{dP}{dt} = \alpha Q - \beta P \tag{8}$$

By writing $a = \alpha + k$ and $R = Q - (RW/a)$, Eq. (7) becomes

$$\frac{dS}{dt} = -aQ + \beta P \tag{9}$$

The standard solutions to the coupled differential equations of Eqs. (8) and (9) are

$$S(t) = C_1 e^{r_1 t} + C_2 e^{r_2 t} \tag{10}$$

$$P(t) = C_1(r_1 - a)e^{r_1 t}/\beta + C_2(r_2 - a)e^{r_2 t}/\beta \tag{11}$$

where r_1 and r_2 are the roots to the characteristic equation

$$\begin{vmatrix} a - r & \beta \\ \alpha & -\beta - r \end{vmatrix} = 0 \tag{12}$$

and C_1 and C_2 are coefficients determined by the boundary conditions. It can be easily shown that r_1 and r_2 are negative numbers, so again Q and P follow the hyperbolic pattern instead of the sigmoidal pattern. In other words, the two-compartment model with recycling can also be rejected by the experimental data with high confidence.

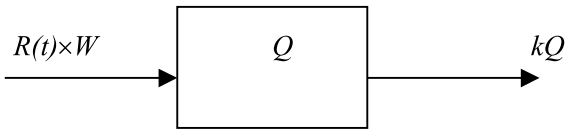

Fig. 5. Single-compartment model with time dependent incorporation rate for the mussel.

3.1.3. One-compartment model with time dependent incorporation rate

We now come to a yet more complicated model, which is a one-compartment model with time dependent incorporation rate (Fig. 5). This model stems from the observation that the curve is similar to the positive substrate cooperativity model. For this model, at low substrate concentrations very few enzyme active sites will have substrate bound to them and they will have a poor affinity for the enzyme, cf., R will be small. When more substrates manage to bind, the positive cooperativity effect increases the ability of the enzyme to bind substrate, cf., R will be large. In other words, R will increase with time at particular exposure periods.

The uptake process is then described by

$$\frac{dQ}{dt} = R(t) \times W - kQ \tag{13}$$

where $R(t)$ is a function of time and is dependent on Q. Without better alternative suggestions, we use the Michaelis–Menten kinetics to describe the relationship between R and Q, i.e.,

$$R = \frac{\gamma Q}{Q + \delta} \tag{14}$$

where γ is the proportionality constant and δ is a parameter equivalent to the Michaelis–Menten constant. For $Q \ll \delta$,

$$R = \frac{\gamma Q}{\delta} \tag{15}$$

and

$$\frac{dQ}{dt} = AQ \tag{16}$$

where

$$A = \gamma W/(\delta - k). \tag{17}$$

If $A > 0$,

$$Q \sim e^{At} \tag{18}$$

which explains the trend at the toe of the sigmoidal curve. Note that for the positive substrate cooperativity to come into effect, A should be greater than zero, or

$$W > \frac{\delta k}{\gamma} \tag{19}$$

Otherwise, A will be negative and Eq. (16) will give a hyperbolic curve instead of an exponentially increasing curve. We will come back to this issue again at the end of the present section. For $Q \gg \delta$,

$$R = \gamma \tag{20}$$

and

$$\frac{dQ}{dt} = \gamma W - kQ \tag{21}$$

which gives the hyperbolic curve described by an equation similar to Eq. (2), which explains the rest of the curve

$$Q = \frac{\gamma W}{k}\left(1 - e^{-kt}\right) + Q_0 e^{-kt} \tag{22}$$

For large exposure time, Q should reach a saturation value given by $\gamma W/k$. Fitting the first three experimental data for 5 ppb Aroclor 1254 to Eq. (18) using the nonlinear curve fitting option of Microcal™ Origin®, and employing inverse of the variances as weights of the data, we found A to be 0.191 ± 0.009 d^{-1}.

The fourth data point has a lower concentration than the third one, which maybe due to experimental uncertainties or other unknown mechanisms. It seems to the authors that the concentration in the mussel for the case for 5 ppb Aroclor 1254 is more likely to saturate at around 408 μg g^{-1} lipid, i.e. $\gamma W/k \approx 408$ μg g^{-1} lipid. From the determined k value of 0.181 d^{-1}, we get $\gamma W = 75.7$ μg g^{-1} lipid d^{-1}. From known values of γW, k and A, we can determine δ from Eq. (17) by

$$\delta = \frac{\gamma W}{A + k} \tag{23}$$

From the above data (for the case 5 ppb Aroclor 1254 in water), we have $\delta \approx 200$ μg g^{-1} lipid. Therefore, the uptake is exponentially increasing when the concentration of PCB in the mussel is small compared to 200 μg g^{-1} lipid, and hyperbolically increasing when the concentration is large compared to 200 μg g^{-1} lipid, which are consistent with the experimental data.

We now return to discuss the criterion for positive substrate cooperativity, viz positive A. In the above example, since $\delta \approx 200$ μg g^{-1} lipid, $k = 0.181$ d^{-1} and $\gamma W = 75.7$ μg g^{-1} lipid d^{-1} (or $\gamma = 15.1$ μg g^{-1} lipid ppb^{-1} d^{-1}), we have $\gamma W > \delta k$ so the condition set out in Eq. (19) holds and A is larger than zero. Therefore, we can see that the conditions in the above example fulfil the criterion for positive substrate cooperativity.

At this point, it is interesting to predict a PCB concentration in water (W) above which the positive substrate cooperativity will come into effect. The critical concentration in water W_c is given by $\gamma W_c = \delta k \approx 36$ μg g^{-1} lipid d^{-1}, so $W_c \approx 2.4$ ppb. This also explains why positive substrate cooperativity does not come into effect for the case 0.5 ppb Aroclor 1254 in water in the previous example.

4. Conclusions

Models for predicting the bioaccumulation of organic chemicals have previously been developed (e.g. Thomann et al., 1992; Gobas, 1993). Despite that these models are simple and more convenient to use, they are equilibrium or static models which have neglected information provided by the dynamic behavior of the bioaccumulation. In other words, these models and thus the inferred underlying bioaccumulation mechanisms are less constrained and are potentially less accurate. Furthermore, in previous models, some important parameters such as the uptake rate (or incorporation rate) and the elimination constant have to be derived from theoretical considerations instead of directly from the experimental data, so the parameters might not reflect accurately the realistic situations.

In the present study, we have found that the single-compartment model with first order kinetics can describe the data for PCB depuration in *P. viridis*. However, the uptake data cannot be satisfactorily explained by this model, or two-compartment models with or without recycling with first order kinetics. The lethal drawback of these models is that they generated hyperbolic uptake curves, which are in contrast to the sigmoidal curves obtained for the experimental uptake data.

Our successful model is a one-compartment model with a time dependent incorporation rate R, with positive substrate cooperativity as the underlying physical mechanism

$$\frac{dQ}{dt} = RW - kQ \tag{24}$$

From the present study, $k = 0.181 \pm 0.017$ d^{-1}. The critical concentration in water W_c is found to be ~2.4 ppb. Below W_c, the positive substrate cooperativity does not come into effect, so R is a constant. For the case of 0.5 ppb Aroclor 1254 in water, $R = 24.0 \pm 2.4$ μg g^{-1} lipid ppb^{-1} d^{-1}. Above W_c, on the other hand, the positive substrate cooperativity will come into effect and R becomes a function of time and dependent on the concentration Q in a form similar to the Michaelis–Menten kinetics

$$R = \frac{\gamma Q}{Q + \delta}$$

where δ is equivalent to the Michaelis–Menten constant. This is the case for 5 ppb Aroclor 1254 in water, where $\gamma = 15.1$ μg g^{-1} lipid ppb^{-1} d^{-1} and $\delta \approx 200$ μg g^{-1} lipid. Therefore, the uptake is exponentially increasing when the concentration of PCB in the mussel is small compared to 200 μg g^{-1} lipid, and hyperbolically increasing when the concentration is large compared to 200 μg g^{-1} lipid, which are consistent with the experimental data.

The model is useful for understanding the true processes taking place during the bioaccumulation and for risk assessment with higher confidence. As mentioned in the introduction, this model is our best model at the moment. Future experimental data which challenge the model are anticipated and desirable for improvement and perfection of the model.

Acknowledgements

The present research was supported by the RGC Central Allocation (CityU reference 8730011) from the Research Grants Council of Hong Kong, and the grant 9360017 for the Centre for Coastal Pollution and Conservation of City University of Hong Kong.

References

Cheung, C.C.C., Zheng, J., Li, A.M.Y., Richardson, B.J., Lam, P.K.S., 2001. Relationships between tissue concentrations of polycyclic aromatic hydrocarbons and antioxidative responses of marine mussels, *Perna viridis*. Aquatic Toxicology 52, 189–203.

Cheung, C.C.C., Zheng, G.J., Lam, P.K.S., Richardson, B.J., in press. Relationships between tissue concentrations of chlorinated hydrocarbons (polychlorinated biphenyls and chlorinated pesticides) and antioxidative responses of marine mussels, *Perna viridis*. Marine Pollution Bulletin.

Connell, D.W., Wu, R.S.S., Richardson, B.J., Leung, K., Lam, P.K.S., Connell, P.A., 1998a. Fate and risk evaluation of persistent organic contaminants and related compounds in Victoria Harbour, Hong Kong. Chemosphere 36, 2019–2030.

Connell, D.W., Wu, R.S.S., Richardson, B.J., Leung, K., Lam, P.K.S., Connell, P.A., 1998b. Occurrence of persistent organic contaminants and related substances in Hong Kong marine areas: an overview. Marine Pollution Bulletin 36, 376–384.

Gobas, F.A.P.C., 1993. A model for predicting the bioaccumulation of hydrophobic organic chemicals in aquatic food-webs: application to Lake Ontario. Ecological Modelling 69, 1–17.

Lam, P.K.S., Gray, J.S., 2001. Predicting effects of toxic chemicals in the marine environment. Marine Pollution Bulletin 42, 169–173.

Martin, M., 1992. California mussel watch: monitoring metal and trace organic toxicants in marine waters. In: Miskiewicz, A.G. (Ed.), Proceedings of a Bioaccumulation Workshop: Assessment of the Distribution, Impacts and Bioaccumulation of Contaminants in Aquatic Environments. Water Board and Australian Marine Sciences Association Inc., Sydney, pp. 15–37.

Phillips, D.J.H., 1985. Organochlorines and trace metals in green-lipped mussels (*Perna viridis*) from Hong Kong waters: a test of indicator ability. Marine Ecology Progress Series 21, 251–258.

Phillips, D.J.H., 1989. Trace metals and organochlorines in the coastal waters of Hong Kong. Marine Pollution Bulletin 20, 319–327.

Prest, H.F., Richardson, B.J., Jocobson, L.A., Vedder, J., Martin, M., 1995. Monitoring organochlorines with semipermeable membrane devices (SPMDs) and mussels *Mytilus edulis* in Corio Bay, Victoria, Australia. Marine Pollution Bulletin 30, 543–554.

Richardson, B.J., Zheng, G.J., Tse, E.S.C., Lam, P.K.S., 2001. A comparison of mussels (*Perna viridis*) and semi-permeable membrane devices SPMDs for monitoring chlorinated trace organic contaminants in Hong Kong coastal waters. Chemosphere 45, 1201–1208.

Sericano, J.L., Wade, T.L., Jackson, T.J., Brooks, J.M., Tripp, B.W., Farrington, J.W., Mee, L.D., Readman, J.W., Villeneuve, J.-P., Goldberg, E.D., 1995. Trace organic contamination in the Americas: an overview of the US National Status and Trends and the international mussel watch programmes. Marine Pollution Bulletin 31, 214–225.

Tanabe, S., Tatsukawa, R., Phillips, D.J.H., 1987. Mussels as bioindicators of PCB pollution: a case study on uptake and release of PCB isomers and congeners in green-lipped mussels (*Perna viridis*) in Hong Kong waters. Environmental Pollution 47, 41–62.

Thomann, R.V., Connolly, J.P., Parkerton, T.F., 1992. An equilibrium model of organic chemical accumulation in aquatic food webs with sediment interaction. Environmental Toxicology and Chemistry 11, 615–629.

Xu, L., Zheng, G.J., Lam, P.K.S., Richardson, B.J., 1999. Relationship between tissue concentrations of polycyclic aromatic hydrocarbons and DNA adducts in green-lipped mussels (*Perna viridis*). Ecotoxicology 8, 73–82.

Yu, K.N., Lam, P.K.S., Ng, K.P., Li, A.M.Y., 2000. Biokinetics of cesium in *Perna viridis*. Environmental Toxicology and Chemistry 19, 271–275.

Zheng, G.J., Lam, M.H.W., Lam, P.K.S., Richardson, B.J., Man, B.K.W., Li, A.M.Y., 2000. Concentrations of persistent organic pollutants in surface sediments of the mudflat and mangroves at Mai Po Marshes Nature Reserve, Hong Kong. Marine Pollution Bulletin 40, 1210–1214.

Zheng, G.J., Quinn, J.G., 1988. Analytical procedures to classify organic pollutants in natural waters, sediments and benthic organisms. Acta Oceanologica Sinica 7, 226–236.